CrystEngComm

PAPER

View Article Online
View Journal | View Issue

Cite this: *CrystEngComm*, 2016, **18**, 7330

Control of the photochromic behavior of cobaloxime complexes with salicylidene-3-aminopyridine and 2-cyanoethyl groups by dual photoisomerization†

Akiko Sekine,* Sayaka Ina, Kohei Johmoto and Hidehiro Uekusa

Received 29th April 2016,
Accepted 10th June 2016

DOI: 10.1039/c6ce01005a

www.rsc.org/crystengcomm

New dual photoisomeric cobaloxime complexes composed of salicylidene-3-aminopyridine derivatives and a 2-cyanoethyl group as axial ligands were synthesized. Photoisomerization of the 2-cyanoethyl group in the crystalline state was performed to control the photochromic properties of the salicylidene-3-aminopyridine derivatives. The colors of the three cobaloxime crystals changed from pale yellow to orange or dark red when the crystals were irradiated with UV light. The red crystals returned to their original color when they were irradiated with visible light or kept in the dark. When the crystals were exposed to visible light before UV irradiation, the 2-cyanoethyl group bonded to the cobalt atom isomerized to the 1-cyanoethyl group with retention of the single crystal form. The crystals containing the 1-cyanoethyl group after photoirradiation also showed photochromism on exposure to UV light. However, the lifetime of the photochromic red species after 2–1 isomerization of the cyanoethyl group was significantly different from that before isomerization. The difference is well explained by the cavity volume around the central C–N bond of the salicylidene moiety in the crystal of the red species.

Introduction

The light-induced reversible color change of materials is called photochromism. Organic photochromic compounds have been applied to optical data storage systems, electronic display systems, optical switching devices, ophthalmic glasses, and so on.[1–4] *N*-Salicylideneanilines (SAs) exhibit photochromism in both solution and the solid state.[5] Photochromic SAs are usually colorless or pale yellow and exist in the *cis*-enol form in crystals, as shown in Scheme 1. The structure of the metastable red species has been controversial for a long time. However, using the crystal of *N*-3,5-di-*tert*-butylsalicylidene-3-nitroaniline, it has been directly confirmed by X-ray analysis with the two-photon excitation technique that the red *trans*-keto form is produced from the *cis*-enol form through the *cis*-keto form, as shown in Scheme 1.[6]

The analyzed structure of the metastable red species shows that a *trans*-keto pair forms around an inversion center with formation of two hydrogen bonds, although no hydrogen bond is observed in the original crystal containing the *cis*-enol form. It has been proposed that these hydrogen bonds may stabilize the metastable *trans*-keto form and the longest lifetime would be realized for the crystal of *N*-3,5-di-*tert*-butylsalicylidene-3-nitroaniline.[7]

For *N*-3,5-di-*tert*-butylsalicylidene-3-carboxyaniline, in which the nitro group in *N*-3,5-di-*tert*-butylsalicylidene-3-nitroaniline is replaced by the carboxyl group, two polymorphic crystals can be obtained (α and β forms) and both show photochromism. The lifetimes of the red species of the α and β forms are 17 and 780 min, respectively, whereas the lifetime of *N*-3,5-di-*tert*-butyl-salicylidene-3-nitroaniline is 1200 min. The crystal structures of the red species of the α and β forms indicate that there is no intermolecular hydrogen bonding in the crystal structure of the red species of the α form, whereas there is one intermolecular hydrogen bond in the red species of the β form.[8] It is clear that the stability of the red species is closely related to the number of intermolecular hydrogen bonds in the crystal of the metastable red species.

To use SAs as photochromic materials, it is very important to control the time of the color change. Although the color

Department of Chemistry and Materials Science, Graduate School of Science and Engineering, Tokyo Institute of Technology, O-okayama, Meguro-ku, Tokyo 152-8551, Japan. E-mail: asekine@chem.titech.ac.jp

† The crystallographic data has been deposited with the Cambridge Crystallographic Data Centre: Deposition numbers CCDC 1476087–1476094 for **I**–**V** and **I′**–**III′**. For crystallographic data in CIF or other electronic format see DOI: 10.1039/c6ce01005a

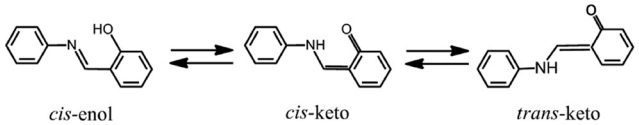

Scheme 1 Photochromic change of *N*-salicylideneaniline.

change time is too fast to control on exposure to UV light, the color change (or fading) time of the red species strongly depends on the intermolecular interactions in the crystal. This suggests that if another photochangeable moiety can be substituted in photochromic SAs, different photochromic behaviors should be observed before and after photoreaction of the inserted moiety. It has been reported that the color of a cobalt complex with a diarylethene derivative ligand changes before and after a methanol molecule coordinates to the cobalt atom under methanol vapor.[9]

Cobaloxime complexes with a photochangeable alkyl group and a base ligand as axial ligands seem to be good candidates to control the photochromic behavior, because they show almost 100% photoisomerization on exposure to visible light without destroying the single crystal form.[10–13] If such a cobaloxime moiety is introduced into a crystal containing SAs, it is expected that the lifetime of the red species of the SA would change before and after the photoisomerization of the alkyl group of the cobaloxime moiety.

In previous studies,[14–16] cobaloxime complexes with a 3-cyanopropyl group and photochromic azobenzene derivatives as an axial alkyl group and base ligands, respectively, were prepared and the photochromic behavior of the azobenzene moiety was compared before and after photoisomerization from the 3-cyanopropyl group to the 1-cyanopropyl group. The rate of the color change because of *trans–cis* isomerization of azobenzene significantly changed. However, it was difficult to investigate how the structural change because of 3–1 photoisomerization influenced the rate of the color change because the crystal gradually decomposed in the process of *trans–cis* isomerization of the azobenzene moiety.

Cobaloxime complexes containing *N*-salicylidene-3-aminopyridines (SAPs), in which the aniline moiety of SAs is replaced by 3-aminopyridine to coordinate to the cobalt atom, have been prepared to control the photochromism of SAP moieties.[17] It was observed that the color fading rates of the SAP moieties significantly changed before and after the 3-cyanopropyl group was isomerized to the 1-cyanopropyl group with retention of the single crystal form on exposure to visible light.

In the present work, the 3-cyanopropyl group is replaced by the 2-cyanoethyl group to determine the effect of a smaller structural change. Five cobaloxime complex crystals with a 2-cyanoethyl group and different axial SAP ligands were prepared: *N*-3,5-di-*tert*-butylsalicylidene-3-aminopyridine (**I**), *N*-3,5-di-*tert*-butylsalicylidene-4-aminopyridine (**II**), *N*-5-methoxysalicylidene-3-aminopyridine (**III**), *N*-5-chlorosalicylidene-3-amino-pyridine (**IV**), and *N*-5-bromosalicylidene-3-aminopyridine (**V**) (Fig. 1). Because photochromism on exposure to UV light was observed for **I–III** but not for **IV** and **V**, the crystal structures of **I–V** were analyzed to determine the reason why the latter two crystals showed no photochromism. Moreover, modified photochromic behavior was observed in **I–III** before and after photoisomerization of the 2-cyanoethyl group. The crystal structures of **I–III** before and after photoisomerization were analyzed. The different photochromic behavior is discussed considering the structural changes during 2–1 photoisomerization.

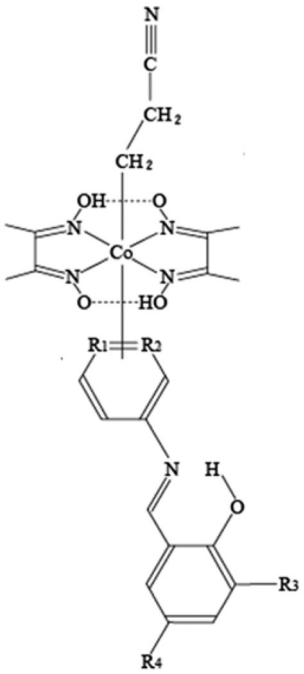

I: R1= C, R2=N, R3=tBu, R4=tBu
II: R1= N, R2=C, R3=tBu, R4=tBu
III: R1= C, R2=N, R3=H, R4=OMe
IV: R1= C, R2=N, R3=H, R4=Cl
V: R1= C, R2=N, R3=H, R4=Br

Fig. 1 Five (2-cyanoethyl)cobaloxime complexes with different axial ligands: **I**: *N*-3,5-di-*tert*-butyl-salicylidene-3-aminopyridine, **II**: *N*-3,5-di-*tert*-butylsalicylidene-4-aminopyridine, **III**: *N*-5-methoxysalicylidene-3-aminopyridine, **IV**: *N*-5-chlorosalicylidene-3-aminopyridine, **V**: *N*-5-bromosalicylidene- 3-aminopyridine.

Experimental

Preparation

(2-Cyanoethyl)(pyridine)cobaloxime. Cobalt(II) chloride hexahydrate (4.77 g, 20 mmol) and dimethylglyoxime (4.68 g) were dissolved in 400 mL of methanol and the solution was stirred for 30 min. An aqueous solution of sodium hydroxide (1.64 g of NaOH in 50 mL of water), 1.6 mL of pyridine, and 2.6 mL of 3-bromopropionitrile were rapidly added to the solution. An aqueous solution of sodium boron hydride (0.78 g of $NaBH_4$ and 150 mL of water) was then slowly added and the solution was kept in the dark for 3 h. The resulting orange solid was washed with water.

***N*-(Salicylidene)-3-aminopyridine derivatives and *N*-(salicylidene)-4-aminopyridine.** 3-Aminopyridine (0.94 g, 10 mmol) was completely melted in a heating mantle at 60 °C, and then an equimolar amount of 3,5-di-*tert*-butylsalicylaldehyde, 5-methoxysalicylaldehyde, 5-chlorosalicylaldehyde, or 5-bromosalicylaldehyde was added. The mixture was then heated and stirred for 2 h at *ca.* 100 °C in an oil bath. The produced oily compound was left

at room temperature overnight. The clumpy crude product was purified by recrystallization from methanol solution at 50 °C. Either *N*-(3,5-di-*tert*-butylsalicylidene)-3-aminopyridine, *N*-5-methoxysalicylidene-3-amino-pyridine, *N*-(5-chlorosalicylidene)-3-aminopyridine, or *N*-(5-bromosalicylidene)-3-aminopyridine was obtained. When equimolar amounts of 4-aminopyridine and 3,5-di-*tert*-butylsalicylaldehyde were used instead of 3-aminopyridine and 3,5-di-*tert*-butylsalicylaldehyde, *N*-(3,5-di-*tert*-butylsalicylidene)-4-aminopyridine was obtained.

Cobaloxime complexes with *N*-(salicylidene)-3-aminopyridine derivatives and *N*-(salicylidene)-4-aminopyridine as axial ligands. (2-Cyanoethyl)(pyridine)cobaloxime (2.18 g) was dissolved in 100 mL of methanol. Water (9 mL) and ion-exchange resin (4.7 g, Dowex 50 W-X8, mesh 50–100, H^+ form) were added and the solution was stirred for 24 h in the dark. After removal of the ion-exchange resin, *N*-3,5-di-*tert*-butylsalicylidene-3-aminopyridine (5 mmol) was added and the solution was stirred at room temperature for 2 h. The crude product (2-cyanoethyl)(*N*-3,5-di-*tert*-butyl-salicylidene-3-aminopyridine)cobaloxime was obtained. (2-Cyanoethyl)-cobaloxime complexes with other salicylidene-3-aminopyridine derivatives and salicylidene-4-aminopyridine as the axial ligands were obtained using the same method. Each powdered sample was dissolved in methanol at 50 °C and kept in the dark. Single yellow or orange crystals of **I–V** were obtained.

Photochromism of I–V owing to UV light irradiation

Each powdered sample of **I–V**, which was obtained by grinding the single crystals, was irradiated with UV light generated by an ultrahigh-pressure Hg lamp (SAN-EI UVF-352S) at room temperature and passed through a glass filter (HOYA UV-360) that allows wavelengths around 360 nm to pass through. The distance between the powdered sample and the lamp was 5 cm. The color of **I** changed from yellow to orange-red, as shown in Fig. 2. The red species thermally faded when the samples were kept in the dark at room temperature or irradiated with visible light. To more quantitatively examine the color change, 7.0 mg of the crystalline powder of each of **I–V** was mixed with 350 mg of barium sulfate in a mortar. The UV/vis spectra of the powdered samples were measured before and after UV irradiation using a JASCO V-560 spectrometer. The absorbance at 500 nm significantly increased because of UV irradiation. The change of the absorbance of **I** is shown in Fig. 3. Similar spectral changes were observed for **II** and **III**. However, no color changes were observed for **IV** and **V**. This suggests that the structural change from the *cis*-enol form to the *trans*-keto form (Scheme 1) occurred in the crystals of **I**, **II**, and **III**, but not in the crystals of **IV** and **V**.

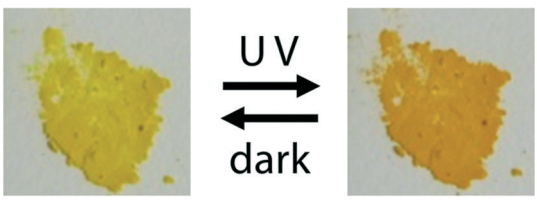

Fig. 2 Color change of I before and after UV irradiation.

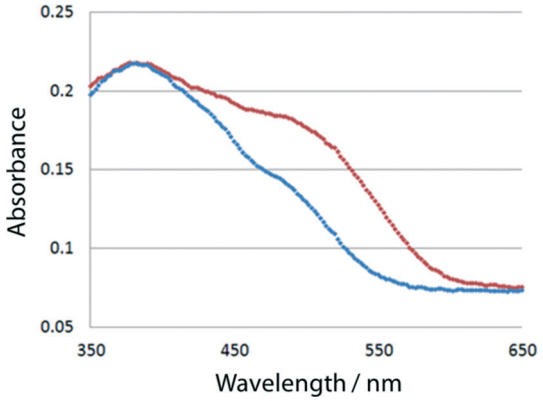

Fig. 3 Change in absorbance of I before (blue) and after 10 sec (red) irradiation.

Isomerization on exposure to visible light

KBr discs (conc. 1.2%) made with powdered samples of **I**, **II**, and **III**, which were obtained by grinding the single crystals, were irradiated with visible light using a xenon lamp (SAN-EI, SUPERBRIGHT-152S), whose top was placed 5 cm from the disc. A glass filter (Toshiba Y44) was inserted between the disc and the lamp. The change in the C≡N stretching vibration was measured at a constant interval with an infrared (IR) spectrometer (Bio-Rad Excalibur FTS 3000). With increasing irradiation time, the peak at *ca.* 2240 cm^{-1} owing to the 2-cyanoethyl group gradually decreased and a new peak owing to the 1-cyanoethyl group appeared at *ca.* 2200 cm^{-1} and then gradually increased. The IR spectra of **I** before and after 120 min irradiation are shown in Fig. 4. This indicates that the 2-cyanoethyl group changed to the 1-cyanoethyl group. The 2–1 isomerization rate exponentially changed in the early stage (<3 min), but the rate gradually decreased and the spectral changes were within the experimental error after 2 h exposure, as shown in Fig. 5.

For powdered samples of **II** and **III**, the changes in the IR spectra were measured in the same way. The isomerization rates in the early stage are somewhat different from that of **I**. The changes became small after 2 h exposure. Although similar 2–1 isomerization was observed for **IV** and **V**, further quantitative measurements were not performed because they showed no photochromism with UV light irradiation.

Photoisomerization of single crystals of I–III

Single crystals of **I**, **II**, and **III** were irradiated with visible light from the xenon lamp through a filter (TOSHIBA, R620) at a distance of 2 cm. This means that the crystal was irradiated with wavelengths longer than 620 nm. 2–1 Isomerization proceeded with retention of the single crystal form. The changes of the cell dimensions of the single crystals of **I**, **II**, and **III** were within the experimental error after 85, 92.5, and

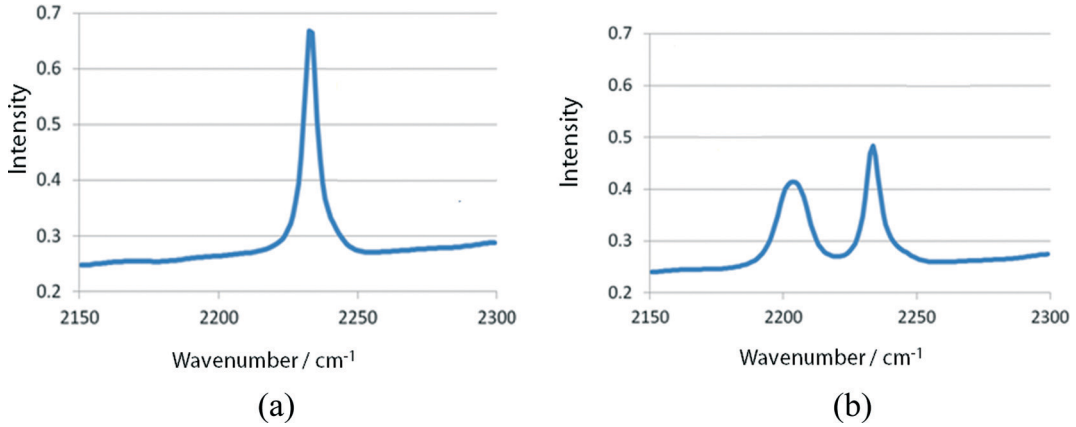

Fig. 4 Change in IR spectra of **I** (a) before and (b) after 120 min visible-light irradiation. The stretching vibration modes of the 2-ce and 1-ce groups appear at 2240 and 2200 cm^{-1}, respectively.

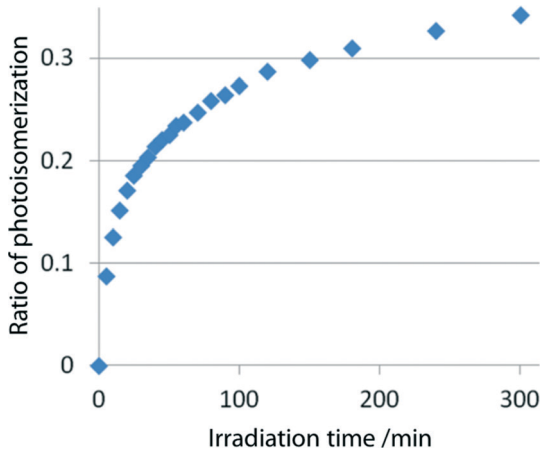

Fig. 5 Rate of the 2–1 photoisomerization of the 2-ce group of **I** at early stages on exposure to visible light.

79 h exposure, respectively. Hereafter, these crystals are called **I′**, **II′**, and **III′**, respectively.

Thermal fading rates

To measure the rate of thermal color fading, time-dependent UV/vis spectra were recorded for the red samples of **I**, **II**, and **III** at intervals of 5 min in the dark at room temperature. The fading rates after time t (min) were obtained from the ratio $(A_t - A_\infty)/(A_0 - A_\infty)$, where A_0 and A_t are the integrated values of the absorbance from 400 to 700 nm at time 0 and time t, respectively, and A_∞ is the corresponding integrated value before irradiation. The rate constant k was determined assuming first-order kinetics using $-kt = \ln[(A_t - A_\infty)/(A_0 - A_\infty)]$ before 2–1 isomerization (before Xe lamp exposure) and after 4 and 15 min irradiation with the lamp, as shown in Fig. 6. The lifetimes of the red species of **I** were obtained by $\tau = 1/k$.

For crystals of **II** and **III**, the lifetimes in the early stage are shown in Fig. 7(a) and (b), respectively. For powdered samples of **I**, **II**, and **III**, the lifetimes of the red species after 2–1 isomerization are shorter, longer, and shorter than the corresponding lifetimes before isomerization, respectively.

Crystal structure analysis

Crystals of **I**–**V** and **I′**–**III′** were mounted on a diffractometer (Rigaku, R-AXIS RAPID or XtalLab) and intensity data was collected with MoKα radiation (λ = 0.71073 Å) at 173(2) K. The crystal data and experimental details for **I**–**III** and **I′**–**III′** are shown in Table 1. The corresponding data for **IV** and **V** are shown in Table 2. Semi-empirical absorption correction was applied. The crystal structures were solved with the program SHELXS97 (ref. 18) or SIR2011 (ref. 19) and refined with full-matrix least-squares on F^2 with the program SHELXL2013.[20] All of the non-hydrogen atoms, including disordered atoms, were refined with anisotropic temperature factors. Hydrogen atoms were obtained geometrically and refined assuming rigid motion with isotropic temperature factors. The non-hydrogen atoms of the minor part of the disordered *tert*-butyl group and the solvent methanol molecule in **I** were refined with isotropic temperature factors. The atoms of the photoproduced 1-cyanoethyl group of **I′** were also refined with isotropic temperature factors. The 2-cyanoethyl and SAP groups of **I**, **II**, and **II′** are disordered. Refinement of the disordered atoms of the 2-cyanoethyl group and the minor part of the SAP group in **II** and **II′** was performed with isotropic temperature factors.

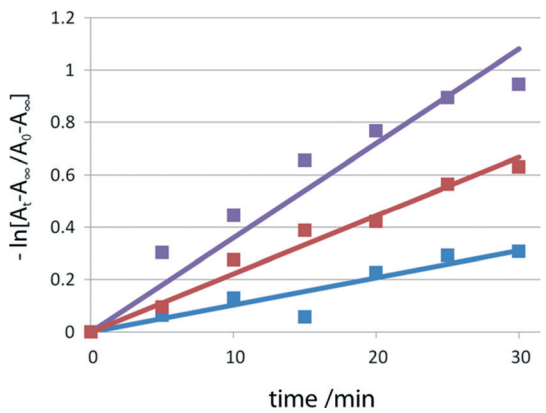

Fig. 6 Fading rates of **I** before visible-light irradiation (blue), and after 4 min (red) and 15 min (violet) irradiation.

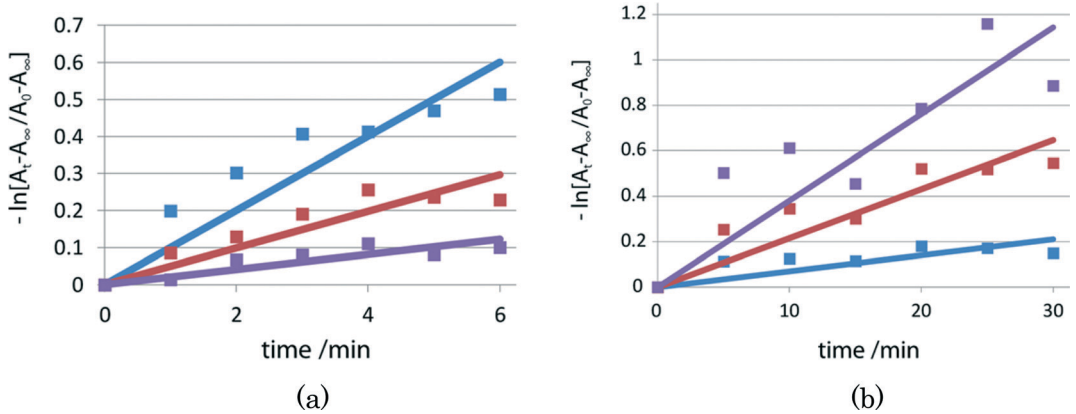

Fig. 7 Fading rates of (a) **II** and (b) **III**. The blue line is before irradiation. The red and violet lines are after 20 and 35 min irradiation in (a), and after 5 and 10 min irradiation in (b), respectively.

Table 1 Crystal data and the experimental details of **I**–**III** and **I′**–**III′**

	I	**I′**	**II**	**II′**	**III**	**III′**
Formula	$C_{31}H_{44}CoN_7O_5$ CH_3OH		$C_{31}H_{44}CoN_7O_5$		$C_{24}H_{30}CoN_7O_6$	
Formula weight	685.70		653.66		571.48	
Crystal system	Monoclinic		Triclinic		Monoclinic	
Space group	$P2_1/n$		$P\bar{1}$		$P2_1/n$	
a (Å)	9.2160(3)	9.1680(6)	8.8800(5)	8.9000(8)	17.2111(5)	17.0830(6)
b (Å)	26.7340(10)	26.964(2)	12.2000(8)	12.2160(12)	7.5620(2)	7.6330(3)
c (Å)	13.9320(5)	14.0240(11)	16.6870(11)	16.8180(15)	21.4770(5)	21.5270(8)
α (°)	90	90	109.096(2)	109.239(3)	90	90
β (°)	96.9100(10)	97.328(2)	95.643(2)	94.666(3)	107.5550(10)	108.7110(10)
γ (°)	90	90	103.792(2)	104.585(3)	90	90
Volume (Å^3)	3408.8(2)	3438.5(4)	1628.16(18)	1643.5(3)	2665.04(12)	2658.65(17)
Z	4		2		4	
D_{calcd} (Mg m^{-3})	1.336	1.325	1.333	1.321	1.424	1.428
Absorp. coeff. (mm^{-1})	0.556	0.551	0.577	0.571	0.696	0.698
F(000)	1456		692		1192	
Crystal size (mm^3)	0.09 × 0.08 × 0.06		0.11 × 0.10 × 0.01		0.36 × 0.13 × 0.10	
Theta range (°)	3.04–27.48	3.02–27.47	3.21–27.42	3.27–27.48	3.01–27.45	3.24–27.47
Index ranges	$-11 \leqq h \leqq 11$	$-10 \leqq h \leqq 11$	$-11 \leqq h \leqq 11$	$-11 \leqq h \leqq 11$	$-22 \leqq h \leqq 22$	$-21 \leqq h \leqq 22$
	$-34 \leqq k \leqq 34$	$-34 \leqq k \leqq 31$	$-15 \leqq k \leqq 15$	$-15 \leqq k \leqq 15$	$-7 \leqq k \leqq 9$	$-9 \leqq k \leqq 9$
	$-18 \leqq l \leqq 17$	$-17 \leqq l \leqq 18$	$-21 \leqq l \leqq 21$	$-20 \leqq l \leqq 21$	$-27 \leqq l \leqq 27$	$-27 \leqq l \leqq 27$
Reflection collected	51 146	30 650	16 072	16 059	24 072	25 059
Independent reflections and R(int)	7797	7531	7365	7371	6055	6059
	0.0988	0.0981	0.0608	0.0948	0.0347	0.0375
Completeness (%)	98.8	95.7	99.1	97.7	99.5	99.4
Max. and min. transmission	0.9674	0.9677	0.9943	0.9943	0.9337	0.9335
	0.6530	0.6532	0.7918	0.7918	0.6807	0.4659
Data/restraints/parameters	7797/2/433	7531/3/451	7365/3/507	7371/4/476	6055/0/351	6059/9/363
Goodness-of-fit on F^2	1.069	1.062	1.023	1.055	1.086	1.099
Final R indices [$I > 2\sigma(I)$]	R_1 = 0.0854	R_1 = 0.0839	R_1 = 0.0569	R_1 = 0.0773	R_1 = 0.0376	R_1 = 0.0491
	wR_2 = 0.1948	wR_2 = 0.1600	wR_2 = 0.1153	wR_2 = 0.1688	wR_2 = 0.0987	wR_2 = 0.1228
R indices (all data)	R_1 = 0.1208	R_1 = 0.1530	R_1 = 0.1029	R_1 = 0.1865	R_1 = 0.0450	R_1 = 0.0590
	wR_2 = 0.2107	wR_2 = 0.1922	wR_2 = 0.1328	wR_2 = 0.2183	wR_2 = 0.1017	wR_2 = 0.1288
Largest diff. peak and hole (e Å^{-3})	1.035	0.611	0.566	0.676	0.795	0.607
	−0.740	−0.629	−0.397	−0.692	−0.348	−0.319

Results and discussion

Crystal and molecular structures of I and I′

The crystal structure of **I** viewed along the a axis is shown in Fig. 8. There is a solvent methanol molecule in the crystal structure. The molecular structure is shown in Fig. 9(a). The 2-cyanoethyl group has a perpendicular conformation, which means that the conformation around the Co–C9–C10–C11 bond is *trans*. The *N*-salicylidene-3-aminopyridine moiety as a whole is nonplanar, but the salicylidene and 3-aminopyridine groups are planar and the dihedral angle between the two planes is 47.8(2)°. One of the two *tert*-butyl groups is disordered, and the occupancy ratio is 82 : 18.

The crystal structure of **I′** is essentially the same as that of **I**, although the unit cell volume is 29.7(2) Å^3 larger. Several new peaks appear around the 2-cyanoethyl group in the

Table 2 Crystal data and experimental details of IV and V

	IV	V
Formula	$C_{23}H_{27}ClCoN_7O_5$	$C_{23}H_{27}BrCoN_7O_5$
Formula weight	575.90	620.36
Crystal system	Monoclinic	Triclinic
Space group	$P2_1$	$P\bar{1}$
a (Å)	7.9620(7)	8.4010(5)
b (Å)	8.4070(6)	13.0930(9)
c (Å)	18.8990(14)	13.7750(10)
α (°)	90	63.746(2)
β (°)	94.566(2)	89.633(2)
γ (°)	90	75.599(2)
Volume (Å^3)	126.02(17)	1306.78(15)
Z	2	2
Density calculated	1.517	1.577
Absorption coeff. (mm^{-1})	0.836	2.233
F(000)	596	632
Crystal size (mm^3)	0.13 × 0.09 × 0.04	0.14 × 0.09 × 0.05
Theta range (°)	3.22–27.42	3.18–27.42
Index ranges (°)	$-10 \leqq h \leqq 10$	$-10 \leqq h \leqq 10$
	$-9 \leqq k \leqq 10$	$-15 \leqq k \leqq 16$
	$-24 \leqq l \leqq 24$	$-17 \leqq l \leqq 17$
Reflection collected	12 560	12 892
Independent reflections and	5130	5881
R(int)	0.1063	0.0740
Completeness (%)	99.7	99.1
Max. and min. transmission	0.9673	0.8965
	0.5285	0.4552
Data/restraints/parameters	5130/1/334	5881/0/331
Goodness-of-fit on F^2	1.069	1.134
Final R indices [$I > 2\sigma(I)$]	R_1 = 0.0639	R_1 = 0.0533
	wR_2 = 0.1209	wR_2 = 0.1151
Final R indices (all data)	R_1 = 0.1306	R_1 = 0.1276
	wR_2 = 0.1644	wR_2 = 0.1605
Largest diff. peak and hole (e Å^{-3})	0.947	1.104
	−0.919	−1.261
Absolute structure parameter	0.03(3)	—

difference electron density map of I′, which are assigned to atoms of the 1-cyanoethyl group. The ratio of the original

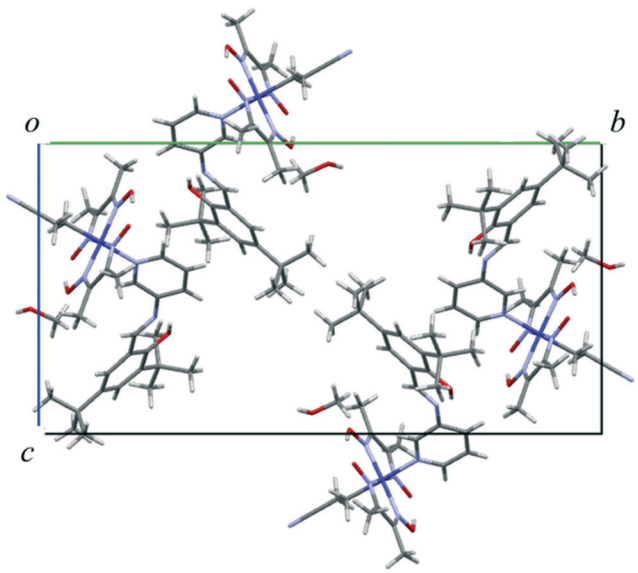

Fig. 8 Crystal structure of I viewed down the *a*-axis. The minor part of the disordered *tert*-butyl groups is omitted for clarity.

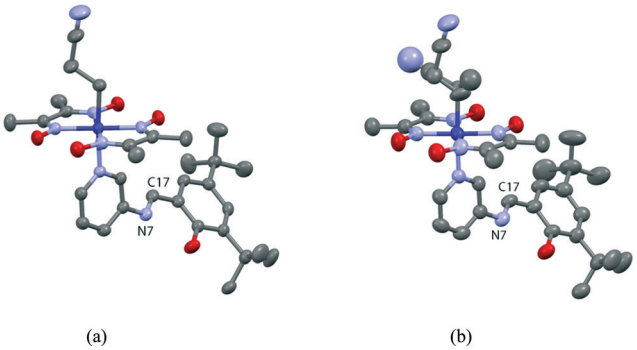

Fig. 9 Major parts of the molecular structures of I before (a) and after (b) visible-light irradiation. The produced 1-cyanoethyl and original 2-cyanoethyl groups take disordered structures in (b). Hydrogen atoms and solvent methanol molecule are omitted for clarity. The thermal ellipsoids of atoms are drawn at the 50% probability level.

2-cyanoethyl group to the produced 1-cyanoethyl group is 58 : 42. The configuration of the 1-cyanoethyl group is limited to *R* or *S* in an asymmetric unit, as shown in Fig. 9(b). The dihedral angle between the salicylidene moiety and the 3-aminopyridine group is 45.8(3)°, which is similar to the original angle. The ratio of the disordered *tert*-butyl group changes to 71 : 29 and the occupancy factor of the solvent methanol molecule significantly decreases.

Crystal and molecular structures of II and II′

The 2-cyanoethyl and SAP groups in the crystal structure of **II** are disordered, as shown in Fig. 10(a). The 2-cyanoethyl group has a perpendicular conformation. The ratios of the major and minor components of the 2-cyanoethyl and SAP groups

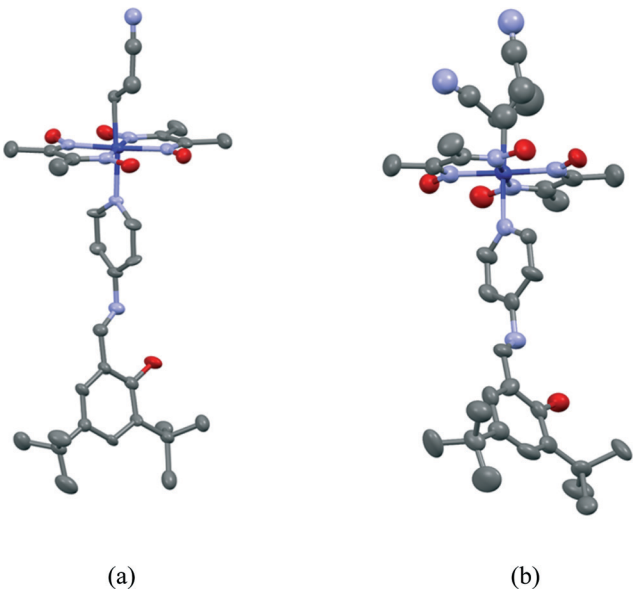

Fig. 10 Molecular structures of II before (a) and after (b) visible-light irradiation. Hydrogen atoms are omitted for clarity. The thermal ellipsoids of atoms are drawn at the 50% probability level. The minor parts of the disordered salicylideneaniline moiety and 2-cyanoethyl group in (a) and the salicylideneaniline moiety in (b) are omitted for clarity.

are 61 : 49 and 69 : 31, respectively. Because the two groups are in close contact in the crystal structure, both groups may be disordered. The dihedral angles between the salicylidene and 3-aminopyridine groups are 88.6(5)° and 77.1(11)° for the major and minor parts of the SAP moiety, respectively.

The crystal structure of **II′** is essentially the same as that of **II**, although the unit-cell volume of **II′** is 15.3(2) Å^3 larger than that of **II**. The 2-cyanoethyl group partly changes to the 1-cyanoethyl group. The molecular structure of **II′** is shown in Fig. 10(b). The ratio of the original 2-cyanoethyl group to the photoproduced 1-cyanoethyl group is 53 : 47. The configuration of the produced 1-cyanoethyl group is only *R* or *S* in an asymmetric unit. The SAP group is also disordered, and the ratio is 69 : 31, which is the same as that of **II**. The dihedral angles between the salicylidene and 3-aminopyridine groups are 85.3(7)° and 71.3(14)° for the major and minor parts, respectively, which are similar to the corresponding angles of **II**.

Crystal and molecular structures of III and III′

The 2-cyanoethyl and SAP groups in the crystal structure of **III** are ordered. The molecular structure of **III** is shown in Fig. 11(a). The 2-cyanoethyl group has a parallel conformation, which means that the conformation around the Co–C9–C10–C11 bond is gauche. There is no short contact between the nitrogen atom of the 2-cyanoethyl group and the N–H group of the salicylidene group. The N–H···N distance is 3.746 or 3.887 Å, which is too long for a weak hydrogen bond.[21] The dihedral angle between the salicylidene and 3-aminopyridine groups is 32.50(9)°.

The crystal structure of **III′** is essentially the same as that of **III**, although the unit-cell volume of **III′** is 6.4(2) Å^3 less than that of **III**. The 2-cyanoethyl group partly changes to the 1-cyanoethyl group. The molecular structure of **III′** is shown in Fig. 11(b). The occupancy factor of the original 2-cyanoethyl group became *ca.* 0.5. The photoproduced 1-cyanoethyl group takes a disordered structure with the *R* and *S* configurations with a ratio of 3 : 2 in an asymmetric unit. No intermolecular hydrogen bonds are formed for the *R* and *S* configurations. The dihedral angle between the salicylidene and 3-aminopyridine groups is 35.90(12)°, which is almost the same as the corresponding angle of **III**.

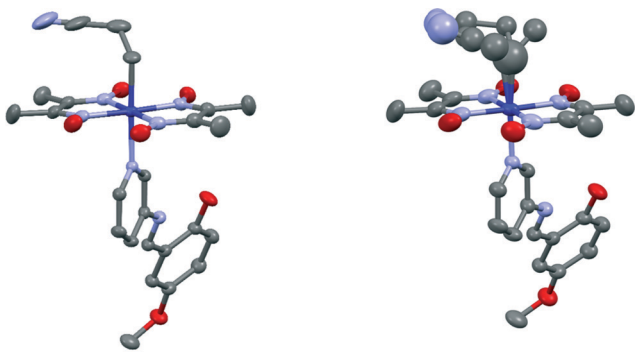

(a) (b)

Fig. 11 Molecular structures of **III** before (a) and after (b) visible light irradiation. Hydrogen atoms are omitted for clarity. The thermal ellipsoids of atoms are drawn at the 50% probability level.

Color fading rates before and after 2–1 isomerization

As shown in Fig. 5 and 6(a) and (b), the lifetimes before and after 2–1 photoisomerization are significantly different, and they are summarized in Table 3. For example, for the powdered sample of **I**, the lifetime of the colored species before 2–1 isomerization is 96 min, but the lifetime gradually decreases on exposure to visible light and the lifetime is 28 min after irradiation with visible light for 15 min. This clearly indicates that the structural change from the 2-cyanoethyl group to the 1-cyanoethyl group decreases the lifetime of the colored species of the SAP molecule coordinated to the cobalt atom from the opposite side of the cobaloxime plane.

For the powdered sample of **II**, the lifetime of the colored species before 2–1 isomerization is 10 min, but it increases to 49 min after the sample was irradiated with visible light for 35 min. The lifetime of the colored species of **III** gradually decrease from 143 min before 2–1 isomerization to 26 min after photoirradiation for 10 min.

Assumed structure of the *trans*-keto form

When single crystals of **I** and **II** were irradiated with visible light, the unit-cell volumes increased by 29.7(2) and 15.3(2) Å^3 at 173 K, respectively. In contrast, the unit-cell volume of **III** decreased by 6.4(2) Å^3 at 173 K. Because the lifetime of colored species strongly depends on the void space in the crystal, it should follow the volume change of the unit cell. However, the unit-cell volume of **III** decreased after 2–1 isomerization, but the lifetime greatly decreased. Therefore, the change of the unit-cell volume has no correlation with the lifetime.

The above results may indicate that intermolecular interactions around the reactive site are the most important factor for the lifetime of the colored species. The structure of the colored species of *N*-3,5-di-*tert*-butylsalicylideneaniline was successfully analyzed using two-photon excitation. The original *cis*-enol form transformed to the *trans*-keto form, as shown in Fig. 12(a). It has been proposed that this transformation should occur through pedal motion of the salicylideneaniline moiety around the central N1–C7 bond.[22] The C4 and C10 atoms occupy nearly the same positions in pedal motion as shown in Fig. 12(b). This means that the void space around the central –N1(H)–C7(H)– group should play

Table 3 Lifetimes of the *trans*-keto forms of **I**, **II** and **III** before and after visible-light irradiation

I		**II**		**III**	
Irradiation time/min	Life time/min	Irradiation time/min	Life time/min	Irradiation time/min	Life time/min
0	96	0	10	0	143
4	45	20	20	5	47
15	28	35	49	10	26

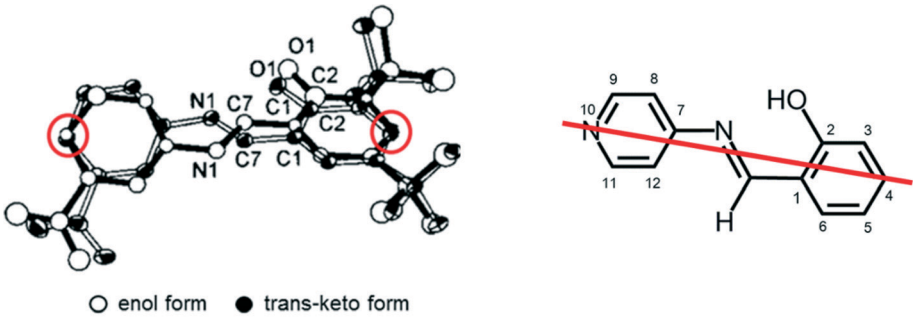

(a) (b)

Fig. 12 (a) Observed structure of the *trans*-keto form of SA,[6] and (b) the model structure of the *trans*-keto form of SAP, assuming that the pedal motion occurs keeping the carbon atom 4 and the nitrogen atom 10 in the same positions.

an important role in the *cis*-enol to *trans*-keto reaction and its back reaction.

Size and shape of the cavity of the *trans*-keto form

To estimate the void spaces around the active sites, the volumes of the cavities around the central –N1(H)–C7(H)– groups of the *trans*-keto forms of **I**, **I′**, **II**, **II′**, **III**, and **III′** were calculated, assuming that the produced *trans*-keto form has the same relative position as the *cis*-enol form observed in each structure. The volumes of the cavities for the *trans*-keto forms of **I** and **I′** are calculated in the same way as those proposed previously[11] and the similar figures of the cavities are drawn in the previous paper.[17] The cavity volumes are 4.1 and 4.5 Å^3 for **I** and **I′**, respectively. The increase in the cavity volume after irradiation suggests a shorter lifetime after 2–1 isomerization than before isomerization, which is consistent with the observed lifetime of **I**.

For the crystal structures of **II** and **II′**, the cavities around the –N1(H)–C7(H)– groups of the assumed *trans*-keto forms were calculated. Because the SAP moieties are disordered in **II** and **II′**, only the major conformation was taken into account. However, similar results were obtained for the minor conformation. The cavity volumes of **II** and **II′** were calculated to be 2.5 and 2.2 Å^3, respectively. These values explain why the lifetime of **II′** (49 min after UV irradiation for 35 min) is significantly longer than that of **II** (10 min).

Conformation effect

For the crystal structures of **III** and **III′**, the cavities around the –N1(H)–C7(H)– groups of the assumed *trans*-keto forms were calculated. The 2-cyanoethyl group in **III** transformed to the 1-cyanoethyl group with *R* and *S* configurations in **III′**, and the *R*/*S* ratio is 29 : 20. The cavity volume for the assumed *trans*-keto form of **III** is 3.0 Å^3. The corresponding cavity volumes of **III′** are 2.5 and 2.6 Å^3 for the *R* and *S* configurations, respectively. This suggests that the lifetime of the *trans*-keto form of **III′** should be longer than that of **III**. However, the lifetimes observed in the experiment were 143 min before irradiation and 26 min after 2–1 isomerization, respectively.

The above results indicate that another factor should be taken into account. In the crystal structure of **III**, there are no effective intermolecular hydrogen bonds. The parallel conformation of the 2-cyanoethyl group may have some influence on the rate of the back reaction. Further experiments should be necessary for the parallel conformation.

Structure of photochromic SAP

It should be clarified why crystals of **IV** and **V** show no photochromism. It has been proposed that salicylideneaniline shows no photochromism if the dihedral angle between the salicylidene and aniline planes is less than 20°. If the dihedral angle is greater than 30°, it shows photochromism. If the dihedral angle is between 20° and 30°, it depends on the crystal structure.[23] The molecular structures of **IV** and **V** are shown in Fig. 13(a) and (b), respectively. The dihedral angles between the planes of the salicylidene moiety and the 3-aminopyridine group are 21.8(4)° and 18.1(3)° for **IV** and **V**, respectively. These values indicate that crystals of **IV** and **V** show no photochromism. Conversely, the corresponding dihedral angles of **I**, **II**, and **III** are 47.8(2)°, 88.6(5)° (major part) and 77.1(11)° (minor part), and 35.90(12)°, respectively. This is a reason why crystals of **I**, **II**, and **III** are photochromic, whereas crystals of **IV** and **V** are non-photochromic. It must be emphasized that although each SAP moiety in the former crystals is coordinated to the cobalt atom of the bulky cobaloxime moiety, it shows a

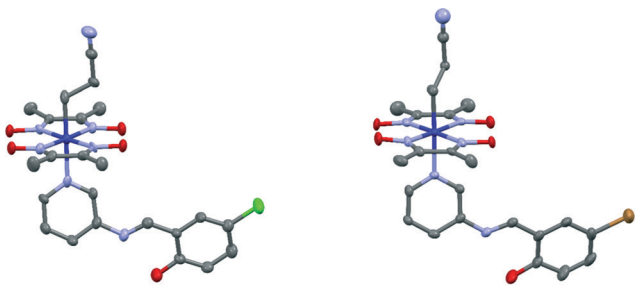

(a) (b)

Fig. 13 Molecular structures of **IV** (a) and **V** (b). Hydrogen atoms are omitted for clarity. The thermal ellipsoids of atoms are drawn at the 50% probability level. The minor part of the 2-cyanoethyl group of **V** is omitted for clarity.

considerably large dihedral angle and therefore the photochromic behavior is conserved.

This work was partly supported by a Grant-in-Aid for Scientific Research in Priority Areas "New Frontiers in Photochromism (no. 471)" given to A. S. by the Ministry of Education, Culture, Sports, Science and Technology (MEXT), Japan. We thank Mr. Yuta Yamazaki for his useful assistance.

References

1 H. Dürr and H. Bouas-Laurent, *Photochromism: Molecules and Systems*, Elsevier, Amsterdam, 2003.
2 J. C. Crano and R. J. Guglielmetti, *Organic Photochromic and Thermochromic Compounds*, vol. 1 and 2, Plenum Press, 1999.
3 M. Irie, *Chem. Rev.*, 2000, **100**, 1685–1716.
4 M. Irie, *Bull. Chem. Soc. Jpn.*, 2008, **81**, 917–926.
5 A. Senier and F. G. J. Shepheard, *J. Chem. Soc., Trans.*, 1909, **95**, 1943–1955.
6 J. Harada, H. Uekusa and Y. Ohashi, *J. Am. Chem. Soc.*, 1999, **121**, 5809–5810.
7 M. Mikami and S. Nakamura, *Phys. Rev. B: Condens. Matter Mater. Phys.*, 2004, **69**, 134205.
8 K. Johmoto, A. Sekine, H. Uekusa and Y. Ohashi, *Bull. Chem. Soc. Jpn.*, 2009, **82**, 50–57.
9 J. Han, M. Maekawa, Y. Suenaga, H. Ebisu, A. Nabei, T. Kuroda-Sowa and M. Munakata, *Inorg. Chem.*, 2007, **46**, 3313–3321.
10 Y. Ohashi and Y. Sasada, *Nature*, 1977, **267**, 142–144.
11 Y. Ohashi, K. Yanagi, T. Kurihara, Y. Sasada and Y. Ohgo, *J. Am. Chem. Soc.*, 1981, **103**, 5805–5812.
12 Y. Ohashi, *Acc. Chem. Res.*, 1998, **21**, 268–274.
13 A. Sekine, H. Tatsuki and Y. Ohashi, *J. Organomet. Chem.*, 1997, **536–537**, 389–398.
14 A. Sekine and Y. Ohashi, *Bull. Chem. Soc. Jpn.*, 1991, **64**, 2183–2187.
15 A. Sekine, H. Yamagiwa and H. Uekusa, *Chem. Lett.*, 2012, **41**, 795–797.
16 H. Yamagiwa and A. Sekine, *Bull. Chem. Soc. Jpn.*, 2013, **86**, 1028–1034.
17 Y. Yamazaki, A. Sekine and H. Uekusa, *Cryst. Growth Des.*, submitted.
18 G. M. Sheldrick, *Acta Crystallogr., Sect. A: Found. Crystallogr.*, 2008, **64**, 112–122.
19 M. C. Burla, R. Caliandro, M. Camalli, B. Carrozzini, G. L. Cascarano, C. Giacovazzo, M. Mallamo, A. Mazzone, G. Polidori and R. Spagna, *J. Appl. Crystallogr.*, 2012, **45**, 357–361.
20 G. M. Sheldrick, *Acta Crystallogr., Sect. A: Found. Adv.*, 2015, **71**, 3–8.
21 G. R. Desiraju and T. Steiner, *The Weak Hydrogen Bond in Structural Chemistry and Biology*, Oxford University Press, New York, 1999.
22 K. Ogawa, T. Sano, S. Yoshimura, Y. Takeuchi and K. Toriumi, *J. Am. Chem. Soc.*, 1992, **114**, 1041–1051.
23 K. Johmoto, T. Ishida, A. Sekine, H. Uekusa and Y. Ohashi, *Acta Crystallogr., Sect. B: Struct. Sci., Cryst. Eng. Mater.*, 2012, **68**, 297–304.

